Journal of the Physical Society of Japan **87**, 024303 (2018)
https://doi.org/10.7566/JPSJ.87.024303

Nonadiabatic Coupling of Molecular States in Presence of Unobserved Perturbers: Modeling and Analysis

Guosheng Feng[1], Feng Xie[2], Vladimir B. Sovkov[1,3*], Jie Ma[1,4†], Liantuan Xiao[1,4], and Suotang Jia[1,4]

[1]*State Key Laboratory of Quantum Optics and Quantum Optics Devices, Institute of Laser Spectroscopy, College of Physics and Electronics Engineering, Shanxi University, Taiyuan, Shanxi 030006, China*
[2]*Institute of Nuclear and New Energy Technology, Collaborative Innovation Center of Advanced Nuclear Energy Technology, Key Laboratory of Advanced Reactor Engineering and Safety of Ministry of Education, Tsinghua University, Beijing, 100084, China*
[3]*St. Petersburg State University, 7/9 Universitetskaya nab., St. Petersburg 199034, Russia*
[4]*Collaborative Innovation Center of Extreme Optics, Shanxi University, Taiyuan, Shanxi 030006, China*

(Received October 7, 2017; accepted December 8, 2017; published online January 15, 2018)

The situation is modeled, in which two electronic states of a diatomic molecule are nonadiabatically coupled to each other as well as to other states, so that levels of the former two states can be registered, while the latter (perturbing) states are unobserved in an experiment. An example being explored is the model of the states $2^3\Pi_g \sim 4^1\Sigma_g^+$ of Rb_2; the computation is done with the multichannel (3-channel, where the third channel represents an effective unobserved perturber) split operator method. Besides the typical resonance-like shifts of a part of the levels, the cases are observed, which cannot be explained within the approximation of a pair–wise resonant interaction. We tested a capability to analyze the synthetic data via an estimate of the interaction matrix element from the magnitudes of the resonance-like shifts combined with an iterative correction of the potential functions, as well as via the two-channel close-coupling calculation.

1. Introduction

In modern molecular spectroscopy, considerable attention is paid to an observation and analysis of excited electronic states of various symmetries, lying noticeably higher above the first dissociation limit.[1–11] They are interesting for a study of the general energetic structure of a molecule, and as the means to investigate the states of the lower dissociation limit.[12–16]

Due to a high density of electronic-vibrational-rotational levels in this region, they exhibit much stronger non-adiabatic effects than the states of the lower limit, so that a considerable portion of the levels are substantially perturbed. This fact complicates their analysis via traditional approaches implying smooth dependencies of energies of the levels on vibrational and rotational quantum numbers, such as those based on the approximations by Dunham[17,18] or by LeRoy and Bernstein.[19–22]

This drawback is rather easily resolved if the character of the coupling is local, so that a mutual interaction within closely spaced pairs of levels governs the principal effect. Properties of such isolated pair–wise interactions are well known: the energetic levels symmetrically repel each other by a value predicted by the secular equation.

In our experience, engaging of experimental intensity data (namely, fluorescence of bound–bound and bound–free transitions to lower electronic states) is very helpful for resolving the problem.[13,15,23]

In cases where the interactions cannot be treated as local and the intensity data are absent or not representative enough, more laborious computational procedures are employed, based on a numerical solution of the multichannel Shrödinger equation considering complete interaction mechanisms.[24–28]

However, even the latter approach can be of questionable success, if the states being observed and analyzed interact significantly with some states, which are not observed in the experiment directly (e.g., the ones not fluorescing in the experimentally accessible wavelength range thanks to selection rules, or just presenting very poor experimental information). On the one hand, inclusion of such states into the computational model is necessary for an adequate accounting of all the interaction mechanisms; on the other hand, there is no enough empirical information on them needed to describe them with an appropriate level of accuracy.

An example of such a situation can be the system $2^3\Pi_g \sim 4^1\Sigma_g^+$ of rubidium dimer. The experimental ro-vibrational term values of the $2^3\Pi_g$ and $4^1\Sigma_g^+$ states were measured in Refs. 15 and 29. To do that, the fluorescence to the lower states ($a^3\Sigma_u^+$, $A^1\Sigma_u^+$) was registered while the frequency of the probe (exciting) laser scanned. Analyses of these data in the cited articles were done (with a partial participation of one of us) separately for every state without explicitly taking into account any non-adiabaticity; however, the results of these analyses clearly showed that these states are strongly coupled to each other as well as to other states of the energetic range.

Inclusion of the total bulk of interactions into the analysis does not look to be possible at the moment as many outer perturbers remain "unobserved", and the entire system is very complicated. Consequently, the question arouse of how much the results can be improved by taking into account the coupling of the two states but ignoring the influence of outer perturbers. It is clear that, any case, a reproduction of the experimental data would improve thanks to a more elaborated model, but this cannot ensure that these results would be physically realistic but not just mathematically artificial.

Based on all these, we came to that at the current stage it would be reasonable to check this circumstance on a simplified synthetic model with known accurate solution, without a pretense to provide a realistic description of the actual molecular states for a while. This is done here.

The purposes of the present work were the modeling of a situation described above and, as far as it was possible, the

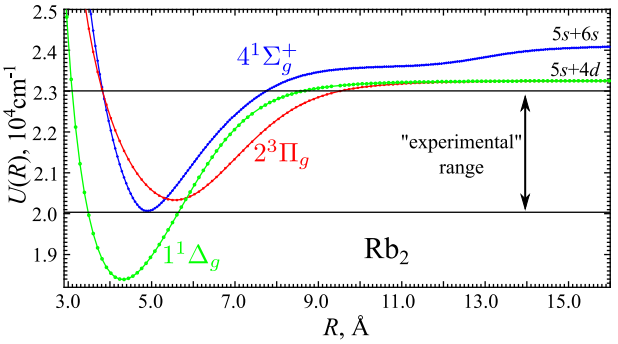

Fig. 1. (Color online) Model diabatic potential functions of Rb_2 $2^3\Pi_g$, $4^1\Sigma_g^+$, and $1^1\Delta_g$ states.

search for a comparably simple approach to an analysis of this problem, including the check of its capability to improve a reproduction of the accurate potential energy functions.

2. Numerical Model

We based our test model on the perturbed system Rb_2 $2^3\Pi_g \sim 4^1\Sigma_g^+$. We decided to imitate the outer perturbations from unobserved states by an interaction with one perturbing electronic state. We have made calculations with several states of Rb_2 in this role. The results have occurred qualitatively similar between each other. Below the results achieved with the $1^1\Delta_g$ perturbing state are presented: this state fairly well spans the energetic region of our interest, and have a rather high density of states within it — see Fig. 1.

We must emphasize that such a model obviously remains rather artificial and very much simplified compared to the actual physical processes in the system. Indeed, if the implied perturbation mechanism is the spin–orbit interaction, then the first-order couplings can only occur between the components $\Omega = 2$ of $2^3\Pi_g \sim 1^1\Delta_g$ and between the components $\Omega = 0$ of $2^3\Pi_g \sim 4^1\Sigma_g^+$, while a transfer of the perturbations between the $\Omega = 0$ and 2 components of the $2^3\Pi_g$ state is only possible via quite indirect higher order mechanisms. Besides, the heterogenic ($\Delta\Omega \neq 0$) matrix elements depend on J,[1)] the effect which was completely neglected by us. In this sense the forces included into our model should be considered effective, i.e., describing a cumulative effect on the "observed" $2^3\Pi_g \sim 4^1\Sigma_g^+$ levels of many complicated mechanisms employing many other states of the energetic region. This approach comply with our purpose to investigate the situation under consideration (how the neglect of unobserved perturbers inflicts the analysis?) using the simplest possible, although more or less realistic, synthetic model without a pretense of describing the actual physics of a system quantitatively.

For the model diabatic potential energy curves we adopted the ab initio potentials.[15,29,30)] The matrix elements of $2^3\Pi_g \sim 4^1\Sigma_g^+$ and $2^3\Pi_g \sim 1^1\Delta_g$ coupling were rather arbitrary taken equal $20\,cm^{-1}$; this generated the shifts of the levels comparable with their experimentally observed scatter; since the direct spin–orbit interaction between the states $1^1\Delta_g$ and $4^1\Sigma_g^+$ is forbidden by a selection rule $\Delta\Lambda \leq 1$, the states $1^1\Delta_g$ and $4^1\Sigma_g^+$ did not interact directly. The diabatic potential energy curves of the model system are shown in Fig. 1; the origin of the energy scale is the bottom of the ground $X^1\Sigma_g^+$ state.

The simulations of the spectra were done with the technique of the multichannel (3-channel in our case) split operator.[31–37)] This is a kind of a so-called pseudo-spectral method, producing an entire spectrum in one time-dependent calculation in a form similar to the experimentally observed one with the regulated spectral resolution. The initial wavepacket in the channels $2^3\Pi_g$ and $4^1\Sigma_g^+$ was formed by a sum of unperturbed stationary wavefunctions with energies $T \leq 23000\,cm^{-1}$ (see Fig. 1 for the "experimental range"), and set to zero in the channel $1^1\Delta_g$. Consequently, the intensities of the lines of the $2^3\Pi_g$ and $4^1\Sigma_g^+$ states became approximately equal to each other, while the state $1^1\Delta_g$ got the status of "unobserved". The unperturbed stationary wavefunctions were computed with the familiar Numerov method.[37–39)]

We computed the non-perturbed (i.e., with the interactions being turned off) and perturbed spectra for the rotational quantum numbers $J = 2, 4, 19, 21, 49, 51$, imitating experimentally observed[15,29)] P and R branches in various excitation schemes. The line energies and their assignments were determined from the synthetic spectra in a manner similar to the analysis of experimental spectra: energies — from the intensity maxima, assignments — based on the requirement of a relative regularity of the energy dependence on the vibrational v and rotational J quantum numbers.

Some characteristic features of the computed spectrum $J = 2$ are shown in Fig. 2.

Figure 2(a) presents an example, where the levels of the $2^3\Pi_g$ and $4^1\Sigma_g^+$ states exhibit a mutual repulsion, which is expected for the local pair–wise (resonant) interaction. This does not mean that they are not perturbed by many other ro-vibrational states, but these perturbations are relatively weak and effectively compensate each other. The effect of the intensity borrowing can be noticed.

The bottom of the $2^3\Pi_g$ well lies near the $4^1\Sigma_g^+$ ($v = 5$) level, so that the lowest levels of the $4^1\Sigma_g^+$ state do not have close neighbors of the $2^3\Pi_g$ symmetry. Nevertheless, they experience the bulk effect (pressure) from all the higher levels of the $2^3\Pi_g$ state, causing their shifts downwards. Figure 2(b) shows the most distant from the $2^3\Pi_g$ level $4^1\Sigma_g^+$ ($v = 0$), whose shift $\sim 0.7\,cm^{-1}$ is quite noticeable.

In Fig. 2(c) the $4^1\Sigma_g^+$ line is repelled from $2^3\Pi_g$, however, in place of the single $2^3\Pi_g$ line the two lines of similar intensities are observed. These two lines represent blended states $2^3\Pi_g \sim 1^1\Delta_g$, so that their assignment to a specific electronic state becomes ambiguous.

The lines shown in Fig. 2(d) exhibit, contrary to the predictions of the pair–wise resonant approximation, not a mutual repulsion but an attraction. The intensity borrowing is also seen.

Thus, as expected, along with the cases, which can be interpreted within a framework of the pair–wise resonant approximation, many examples are observed, where the positions and intensities of ro-vibrational lines are significantly influenced by energetically distant levels of the observed partner, as well as by levels of an unobserved electronic state.

3. Analysis

Our desire was to find and check such approaches to an analysis of a set of perturbed ro-vibrational term values in

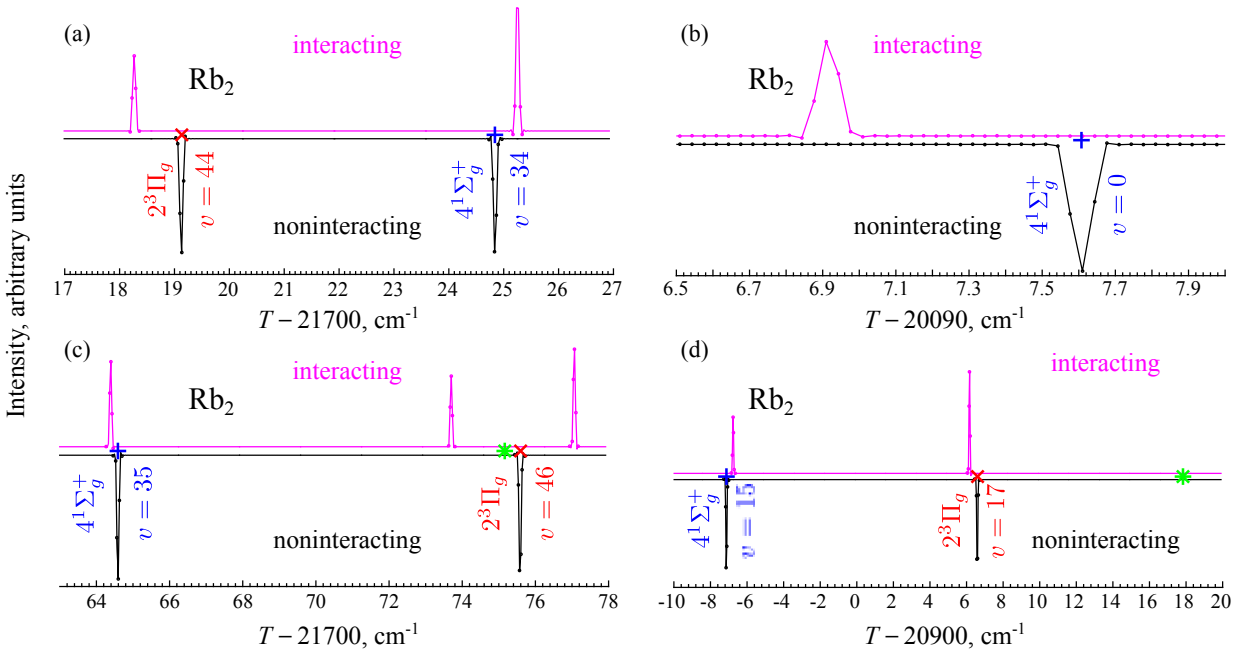

Fig. 2. (Color online) Examples of characteristic perturbational features (upper) in comparison with the unperturbed lines (lower) in the model spectra of the Rb_2 $2^3\Pi_g \sim 4^1\Sigma_g \sim 1^1\Delta_g$ system; unperturbed levels belong to the states: (+)–$4^1\Sigma_g^+$, (×)–$2^3\Pi_g$, (∗)–$1^1\Delta_g$.

presence of an unobserved perturber, which would avoid addressing any experimentally unconfirmed information on the unobserved state. Below we describe such approaches and test them for the set of synthetic experimental data from the previous section of the article.

At our first approach, we relied on a supposition, that there existed a group of levels, which could be described within an approximation of the pair–wise resonant interaction with an adequate accuracy [see Fig. 2(a)]. Their selection out of the entire multitude of the registered levels would allow us to estimate the coupling matrix elements, and then update the potential energy curves iteratively.

Notice, that an attempt to include into this system the third perturbing level does not make much sense: three isolated levels is a rare event; besides, if even such an event occurs, it is unclear of how to separate this group containing an unobserved state from other levels.

Within the approximation of the pair–wise resonant interaction, the energies T_1, T_2 of the mutually perturbed levels are the solutions of the secular equation

$$\det\begin{pmatrix} T_1^{(0)} - T & W_{12} \\ W_{12} & T_2^{(0)} - T \end{pmatrix} = 0, \tag{1}$$

where $T_1^{(0)}$, $T_2^{(0)}$ are the non-perturbed eigenenergies, $W_{12} = \langle 1|W|2\rangle$ is the interaction matrix element, W is the electronic matrix element. Solving this equation for W_{12}, we get the expressions:

$$W_{12}^{(a)} = \sqrt{(T_1^{(0)} - T_1)(T_2^{(0)} - T_1)} = \sqrt{(T_1^{(0)} - T_1)^2 + (T_2^{(0)} - T_1^{(0)})(T_1^{(0)} - T_1)}\,, \tag{2}$$

$$W_{12}^{(b)} = \sqrt{(T_1^{(0)} - T_2)(T_2^{(0)} - T_2)} = \sqrt{(T_2^{(0)} - T_2)^2 + (T_1^{(0)} - T_2^{(0)})(T_2^{(0)} - T_2)}\,, \tag{3}$$

enabling to estimate the coupling matrix element W_{12} from the hypothetical unperturbed term values $T_1^{(0)}$, $T_2^{(0)}$ and at least one of the experimental term values T_1, T_2. The formulae (2) and (3) can produce different results if $|T_2^{(0)} - T_2| \neq |T_1^{(0)} - T_1|$, which might happen either if the approximation of the pair–wise resonant interaction breaks or if the hypothetical non-perturbed eigenenergies $T_1^{(0)}$, $T_2^{(0)}$ are not adequate. The first effect is partly canceled out by adopting the mean value of the two estimates:

$$W_{12}^{(ab)} = \frac{1}{2}(W_{12}^{(a)} + W_{12}^{(b)}). \tag{4}$$

The second effect can be overcome by a correction of the zero-th approximation in such a way as the empirical estimate of the matrix element $W_{12}^{(ab)}$ to accord its quantum-mechanical prediction $\langle 1|W|2\rangle$.

The potentials $U(R)$ (R is the atomic separation) were modeled by the functions:[40–43]

$$U(R) = E_D + \begin{cases} U_{IR}(R), & R_{SR} \le R \le R_{LR}, \\ U_{SR}(R), & R < R_{SR}, \\ U_{LR}(R), & R > R_{LR}, \end{cases} \tag{5}$$

$$U_{IR}(R) = \sum_{i=0}^{N} a_i \xi^i(R), \quad \xi = \frac{R - R_m}{R + \alpha R_m},$$

$$U_{SR}(R) = u_1 + u_2/R^{N_s},$$

$$U_{LR}(R) = -\sum_{i=1}^{L} C_{N_i}/R^{N_i}.$$

The values at the dissociation limits were chosen (from the atomic asymptotes) $E_D = 23349\,\mathrm{cm}^{-1}$ ($2^3\Pi_g$) and $E_D = 24126\,\mathrm{cm}^{-1}$ ($4^1\Sigma_g^+$); the values of the long-range asymptote powers $N_1 = 6$ and $N_2 = 8$; the value of the short-range asymptote power $N_s = 4.5$; the coefficients u_1, u_2, C_6, C_8 were computed so as to ensure the continuity of the function and its first derivative. However, all the synthetic experimental term values lie within the middle part $U_{IR}(R)$ of the potential functions and are not almost influenced by the

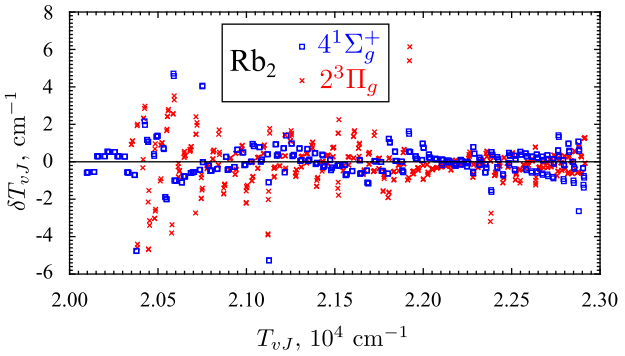

Fig. 3. (Color online) Residuals of the final simulation with the pair–wise deperturbation approach of the synthetic experimental ro-vibrational term values T_{vN} in the model spectra of the Rb_2 $2^3\Pi_g \sim 4^1\Sigma_g \sim 1^1\Delta_g$ system.

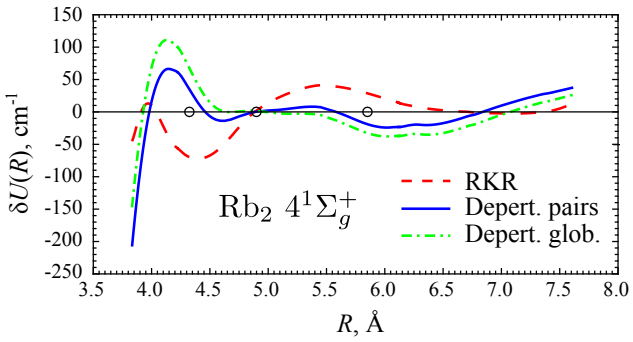

Fig. 4. (Color online) Accuracy of the potential function determination with the RKR (dashed), pair–wise deperturbation (solid), and global 2-channel deperturbation (point-dashed) methods for the Rb_2 $4^1\Sigma_g^+$ state; circles indicate postions of the potential minimum and of 1/4 depth of the well.

asymptotic parts, which thereby play a pure technical role in computational algorithms.

At the zero-th step we computed the Rydberg–Klein–Rees (RKR)[37,44–47] potentials and approximated them with Eq. (5). After that, parameters a_i, α, R_m were optimized within the following iterative procedure.

(1) Current approximations for the $2^3\Pi_g$ and $4^1\Sigma_g^+$ potential functions were constructed in the form of Eq. (5).
(2) The unperturbed eigenenergies $T^{(0)}_{v_1J_1}$, $T^{(0)}_{v_2J_2}$ and wave-functions $\Psi^{(0)}_{v_1J_1}$, $\Psi^{(0)}_{v_2J_2}$ were computed with the Numerov method.[37–39]
(3) For every J the resonance-like pairs of neighboring levels (v_1, v_2) were found and selected (i.e., those which repel each other).
(4) For every selected pair (v_1, v_2) the matrix element $W^{(ab)}_{v_1v_2,J}$ was estimated with Eqs. (2)–(4).
(5) For every selected pair (v_1, v_2) the overlap integral

$$w_{v_1v_2,J} = |\langle \Psi^{(0)}_{v_1,J}(R) | \Psi^{(0)}_{v_2,J}(R) \rangle|$$

was computed.
(6) The interaction constant W was estimated as a mean value of $W^{(ab)}_{v_1v_2,J}/w_{v_1v_2,J}$ over all the selected pairs (v_1, v_2).
(7) The evaluation (objective) function was constructed from the squares of the residuals $T_1 - T^{(0)}_1$, $T_2 - T^{(0)}_2$, and $W^{(ab)}_{v_1v_2,J} - W \cdot w^{(ab)}_{v_1v_2,J}$.
(8) The parameters of the model were corrected by minimizing the evaluation function with the Levenberg–Marquardt algorithm.[37,48]

The residuals of the final reproduction of the synthetic experimental term values are shown in Fig. 3.

The resulting estimate of the interaction constant was $W = 28\,\mathrm{cm}^{-1}$ (recall that the accurate model value had been $W = 20\,\mathrm{cm}^{-1}$).

Along with the algorithm described above, we tried a direct fit of the synthetic experimental term values with the global two-channel $2^3\Pi_g \sim 4^1\Sigma_g^+$ close-coupling computation performed with the Fourier grid method.[9,11,37,49–51] This resulted in the interaction constant of $W = 17.5\,\mathrm{cm}^{-1}$. Quite expectedly, the reproduction of the synthetic experimental term values improved (mean square error $0.82\,\mathrm{cm}^{-1}$ vs $1.03\,\mathrm{cm}^{-1}$).

The errors of the final reproduction of the accurate model potential functions with the both approaches are shown

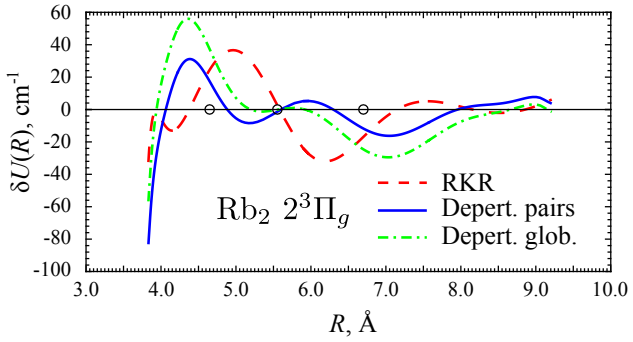

Fig. 5. (Color online) Accuracy of the potential function determination with the RKR (dashed), pair–wise deperturbation (solid), and global 2-channel deperturbation (point-dashed) methods for the Rb_2 $2^3\Pi_g$ state; circles indicate postions of the potential minimum and of 1/4 depth of the well.

in Figs. 4 and 5 in comparison with the straightforward RKR[37,44–47] potentials.

4. Discussion

The results of the analysis can be accepted as a satisfactory zero-th order approximation. The estimates of the coupling constant are at least reasonable. The potential functions exhibit a definite improvement over the RKR curves in the regions of the potential well bottoms, but worsen at higher energies, especially at the left walls, whose influence on the simulations is relatively weak.[19–22] The overall qualities of the potential functions found with the method exploiting the resonance-like pairs and the one based on the two-channel close-coupling simulation are similar to each other. However, an improvement over the RKR curves does not look crucial. For a better result an inclusion of the unobserved states into the computational model looks to be necessary.

We would also like to emphasize, that the potential energy functions of the Rb_2 $2^3\Pi_g$ and $4^1\Sigma_g^+$ states reported in Refs. 15 and 29 remain their best descriptions available for the moment.

5. Conclusions

The problem of the analysis of nonadiabatically coupled molecular states in presence of unobserved perturbers is

proponed. The model of the coupled states $2^3\Pi_g$, $4^1\Sigma_g^+$, $1^1\Delta_g$ of rubidium dimer is investigated as an example. The characteristic perturbational features are simulated. Algorithms to analyze such systems are tested, where no information on the unobserved state is addressed. The outcome of these approaches can be accepted as a reasonable zero-th approximation. The work illustrates what can be expected from the analysis of nonadiabatically coupled molecular states neglecting an influence of unobserved perturbers.

Acknowledgements This work was supported by the National Key Research and Development Program of China (Grant No. 2017YFA0304203), the Changjiang Scholars and Innovative Research Team in the University of the Ministry of Education of China (Grant No. IRT13076), the National Natural Science Foundation of China (Grant Nos. 61722507, 61675121, 61705123, and 11434007), the fund for Shanxi "1331 Project" Key Subjects Construction, the foundation for Outstanding Young Scholars of Shanxi Province, China (Grant No. 201601D021001), and the Fund Program for the Scientific Activities of Selected Returned Overseas Professionals in Shanxi Province (Grant No. 2017-07).

*v.sovkov@spbu.ru
†mj@sxu.edu.cn

1) H. Lefebvre-Brion and R. W. Field, *The Spectra and Dynamics of Diatomic Molecules* (Elsevier Academic Press, Amsterdam-Boston-Heidelberg-New York-Oxford-Paris-San Diego-San Francisco-Singapore-Sydney-Tokio, 2004).
2) W. C. Stwalley, J. Mol. Spectrosc. **330**, 14 (2016).
3) L. Li and R. W. Field, J. Phys. Chem. **87**, 3020 (1983).
4) P. Yi, X. Dai, J. Li, Y. Liu, L. Li, V. B. Sovkov, and V. S. Ivanov, J. Mol. Spectrosc. **225**, 33 (2004).
5) F. Xie, D. Li, Y. Chu, L. Li, S. Magnier, V. B. Sovkov, and V. S. Ivanov, J. Phys. Chem. A **110**, 11260 (2006).
6) Z. Chena, C.-z. Cui, Y.-m. Liu, L. Li, V. B. Sovkov, and V. S. Ivanov, Chin. J. Chem. Phys. **19**, 11 (2006).
7) F. Xie, D. Li, L. Tyree, L. Li, V. B. Sovkov, V. S. Ivanov, S. Magnier, and A. M. Lyyra, J. Chem. Phys. **128**, 204313 (2008).
8) J. Ma, W. Liu, J. Yang, J. Wu, W. Sun, V. S. Ivanov, A. S. Skublov, V. B. Sovkov, X. Dai, and S. Jia, J. Chem. Phys. **141**, 244310 (2015).
9) W. Liu, R. Xu, J. Wu, J. Yang, S. S. Lukashov, V. B. Sovkov, X. Dai, J. Ma, L. Xiao, and S. Jia, J. Chem. Phys. **143**, 124307 (2015).
10) J. Yang, Y. Guan, W. Zhao, Z. Zhou, X. Han, J. Ma, V. B. Sovkov, V. S. Ivanov, E. H. Ahmed, A. M. Lyyra, and X. Dai, J. Chem. Phys. **144**, 024308 (2016).
11) W. Liu, J. Wu, J. Ma, P. Li, V. B. Sovkov, L. Xiao, and S. Jia, Phys. Rev. A **94**, 032518 (2016).
12) F. Xie, V. B. Sovkov, A. M. Lyyra, D. Li, S. Ingram, J. Bai, V. S. Ivanov, S. Magnier, and L. Li, J. Chem. Phys. **130**, 051102 (2009).
13) F. Xie, L. Li, D. Li, V. B. Sovkov, K. V. Minaev, V. S. Ivanov, A. M. Lyyra, and S. Magnier, J. Chem. Phys. **135**, 024303 (2011).
14) B. Beser, V. B. Sovkov, J. Bai, E. H. Ahmed, C. C. Tsai, F. Xie, L. Li, V. S. Ivanov, and A. M. Lyyra, J. Chem. Phys. **131**, 094505 (2009).
15) Y. Guan, X. Han, J. Yang, Z. Zhou, X. Dai, E. H. Ahmed, A. M. Lyyra, S. Magnier, V. S. Ivanov, A. S. Skublov, and V. B. Sovkov, J. Chem. Phys. **139**, 144303 (2013).
16) J. A. Lau, J. P. Toennies, and K. T. Tang, J. Chem. Phys. **145**, 194308 (2016).
17) J. L. Dunham, Phys. Rev. **41**, 713 (1932).
18) J. L. Dunham, Phys. Rev. **41**, 721 (1932).
19) R. J. LeRoy and R. B. Bernstein, J. Chem. Phys. **52**, 3869 (1970).
20) D. Comparat, J. Chem. Phys. **120**, 1318 (2004).
21) V. B. Sovkov and V. S. Ivanov, J. Chem. Phys. **140**, 134307 (2014).
22) V. B. Sovkov and V. S. Ivanov, St. Petersburg University. Ser. 4. **1** [59], 473 (2004).
23) V. S. Ivanov, V. B. Sovkov, N. Gallice, L. Li, Y. Liu, A. M. Lyyra, and S. Magnier, J. Mol. Spectrosc. **209**, 116 (2001).
24) M. R. Manaa, A. J. Ross, F. Martin, P. Crozet, A. M. Lyyra, L. Li, C. Amiot, and T. Bergeman, J. Chem. Phys. **117**, 11208 (2002).
25) P. Qi, J. Bai, E. Ahmed, A. M. Lyyra, S. Kotochigova, A. J. Ross, C. Effantin, P. Zalicki, J. Vigué, G. Chawla, R. W. Field, T. J. Whang, W. C. Stwalley, H. Knöckel, E. Tiemann, J. Shang, L. Li, and T. Bergeman, J. Chem. Phys. **127**, 044301 (2007).
26) H. Salami, T. Bergeman, B. Beser, J. Bai, E. H. Ahmed, S. Kotochigova, A. M. Lyyra, J. Huennekens, C. Lisdat, A. V. Stolyarov, O. Dulieu, P. Crozet, and A. J. Ross, Phys. Rev. A **80**, 022515 (2009).
27) J. Bai, E. H. Ahmed, B. Beser, Y. Guan, S. Kotochigova, A. M. Lyyra, S. Ashman, C. M. Wolfe, J. Huennekens, F. Xie, D. Li, L. Li, M. Tamanis, R. Ferber, A. Drozdova, E. Pazyuk, A. V. Stolyarov, J. G. Danzl, H. C. Nägerl, N. Bouloufa, O. Dulieu, C. Amiot, H. Salami, and T. Bergeman, Phys. Rev. A **83**, 032514 (2011).
28) A. N. Drozdova, A. V. Stolyarov, M. Tamanis, R. Ferber, P. Crozet, and A. J. Rose, Phys. Rev. A **88**, 022504 (2013).
29) X. Han, J. Yang, Y. Guan, Z. Zhou, W. Zhao, A. R. Allouche, S. Magnier, E. Ahmed, A. Lyyra, and X. Dai, Chem. Phys. Lett. **601**, 124 (2014).
30) A. R. Allouche and M. Aubert-Frécon, J. Chem. Phys. **136**, 114302 (2012).
31) M. D. Feit, J. A. Fleck, Jr., and A. Steiger, J. Comput. Phys. **47**, 412 (1982).
32) M. D. Feit and J. A. Fleck, Jr., J. Chem. Phys. **78**, 301 (1983).
33) V. S. Ivanov, V. N. Serov, and V. B. Sovkov, in *Abstracts of 31 Conf. "European Group on Atomic Spectroscopy"*, ed. F. Vedel (European Physical Society, Marseille, France, 1999) p. 267.
34) V. S. Ivanov, V. N. Servo, and V. B. Sovkov, in *Book of Abstracts: The 16th Int. Conf. High Resolution Molecular Spectrocopy*, ed. O. Bludský, P. Pracna, V. Špirko, and Š. Urban (J. Heyrovský Institute of Physical Chemistry of Academy of Sciences of the Czech Republic, Prague, Czech Republic, 2000) p. 48.
35) V. N. Serov, V. B. Sovkov, V. S. Ivanov, and O. Atabek, J. Chem. Phys. **115**, 6450 (2001).
36) V. S. Ivanov and V. B. Sovkov, in *Book of Abstracts: The 17th Int. Conf. High Resolution Molecular Spectrocopy*, ed. O. Bludský, P. Pracna, V. Špirko, Š. Urban, and Z. Zelinger (Institute of Chemical Technology, Prague, Czech Republic, 2002) p. 143.
37) V. B. Sovkov and J. Ma, in *Proc. 2016 Int. Conf. Applied Mathematic Simulation and Modelling, Advances in Computer Science Research*, ed. A. Dadvand, K. Nagaraja, and Mirzazadeh (Atlantis Press, Beijing, China, 2016) p. 369.
38) J. M. Blatt, J. Comput. Phys. **1**, 382 (1967).
39) R. J. Le Roy, J. Quant. Spectrosc. Radiat. Transfer **186**, 167 (2017).
40) C. Samuelis, E. Tiesinga, T. Laue, M. Elbs, H. Knöckel, and E. Tiemann, Phys. Rev. A **63**, 012710 (2000).
41) A. Pashov, O. Docenko, M. Tamanis, R. Ferber, H. Knöckel, and E. Tiemann, Phys. Rev. A **76**, 022511 (2007).
42) C. Strauss, T. Takekoshi, F. Lang, K. Winkler, R. Grimm, J. H. Denschlag, and E. Tiemann, Phys. Rev. A **82**, 052514 (2010).
43) V. B. Sovkov, V. S. Ivanov, K. V. Minaev, and M. S. Aleksandrov, Opt. Spectrosc. **114**, 167 (2013).
44) R. Rydberg, Z. Phys. **73**, 376 (1932).
45) R. Rydberg, Z. Phys. **80**, 514 (1933).
46) O. Klein, Z. Phys. **76**, 226 (1932).
47) A. L. G. Rees, Proc. Phys. Soc. London **59**, 998 (1947).
48) D. W. Marquardt, J. Soc. Ind. Appl. Math. **11**, 431 (1963).
49) C. C. Marston and G. G. Balint-Kurti, J. Chem. Phys. **91**, 3571 (1989).
50) V. Kokoouline, O. Dulieu, R. Kosloff, and F. Masnou-Seeuws, J. Chem. Phys. **110**, 9865 (1999).
51) K. Willner, O. Dulieu, and F. Masnou-Seeuws, J. Chem. Phys. **120**, 548 (2004).